

# Supporting Information

## Gold Nanoparticle-Induced Cell Death: Solid Gold Nanospheres versus Hollow Gold Nanocages

Megan A. Mackey, Farhat Saira, Mahmoud A. Mahmoud, and Mostafa A. El-Sayed\*

*Laser Dynamics Laboratory, School of Chemistry and Biochemistry, Georgia Institute of  
Technology, Atlanta, Georgia, USA*

\*Corresponding author: Mostafa A. El-Sayed, 901 Atlantic Drive, Atlanta, Georgia,  
30332-0400, USA. phone: 404-894-0292, fax: 404-894-7452, email:

[melsayed@gatech.edu](mailto:melsayed@gatech.edu)

### Table of contents:

#### Page 2

Table S1: Zeta potential measurements for the various nanoparticles used in this work

#### Page 3

Figure S1: Confocal microscopy images of RGD/NLS-AuNCs and RGD/NLS-AuNSs in HSC cells

#### Page 4

Figure S2: HSC cell cycle analysis of RGD conjugated AuNCs and AuNSs, and NLS conjugated AuNCs and AuNSs

#### Page 5

Figure S3: HSC cell cycle histograms obtained from raw flow cytometry data

#### Page 6

Figure S4: HSC cell death induced by RGD conjugated AuNCs and AuNSs, and NLS conjugated AuNCs and AuNSs

#### Page 7

Figure S5: ROS generated in HSC cells by RGD conjugated AuNCs and AuNSs, and NLS conjugated AuNCs and AuNSs

#### Page 8

Figure S6: HaCat cell death induced by all nanoparticle formulations tested on the HSC cells

#### Page 9

Figure S7: UV-Vis spectra showing a redshift in the surface plasmon resonance of AuNCs in cell culture medium after 48 h

**Table S1.** Zeta potential measurements for functionalized AuNSs and AuNCs used throughout this study.

	zeta potential (mV)	<u>±</u>
PEG-AuNSs	-11	2
NLS-AuNSs	-2	3
RGD-AuNSs	-4	3
RGD/NLS-AuNSs	1	3
PEG-AuNCs	-10	2
NLS-AuNCs	2	2
RGD-AuNCs	-1	3
RGD/NLS-AuNCs	-3	1

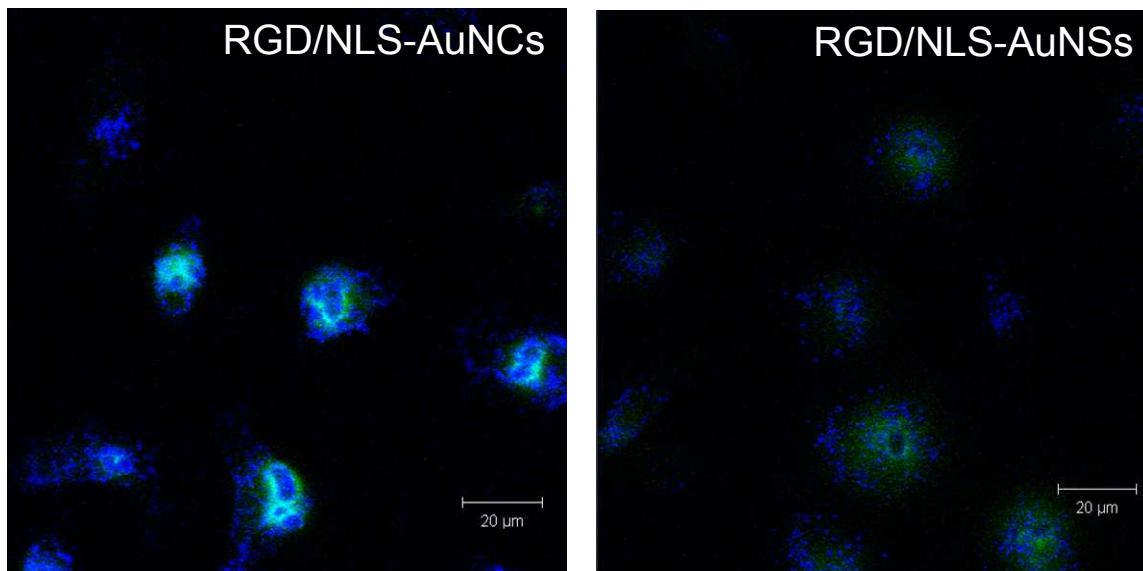


**Figure S1.** Confocal microscopy images of FITC (green) labeled RGD/NLS-AuNCs (left) and AuNSs (right) co-localized with the nuclei (blue) of HSC cells. For FITC labeling, nanoparticles were conjugated with FITC-PEG-SH prior to peptide conjugation. After nanoparticle functionalization, HSC cells were prepared for confocal imaging. Briefly, HSC-3 cells were grown on coverslips overnight. The growth media was then removed and replaced with growth media containing FITC-RGD/NLS-AuNCs and AuNSs. After a 24 h incubation period with gold nanoparticles, the gold nanoparticle-containing media was removed and the cells were washed with PBS. Cells were then fixed with 4% paraformaldehyde for 15 min, followed by nuclear staining with DAPI (4',6-Diamidino-2-phenylindole, Dihydrochloride, Invitrogen) and washing with water. Fluorescence images were taken by multiphoton confocal microscopy using the Zeiss LSM 510 NLS META with 785 (DAPI) and 488 nm (FITC) excitation sources. Scale bar: 20  $\mu\text{m}$ .

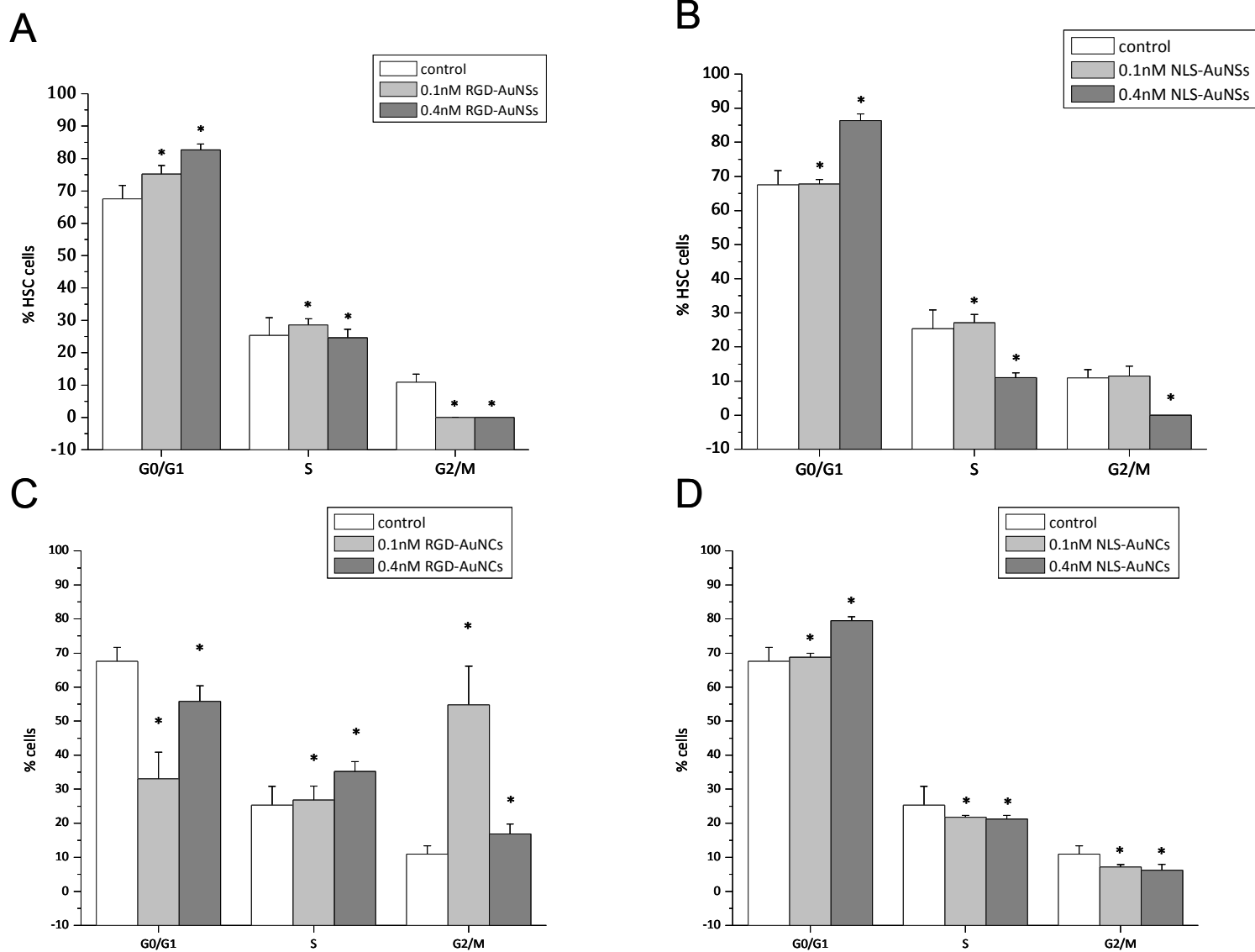


**Figure S2.** Cell cycle changes induced by 0.1 and 0.4 nM peptide-conjugated gold nanoparticles in HSC cells after 48 h treatment with RGD-AuNSs (A), NLS-AuNSs (B), RGD-AuNCs (C) and NLS-AuNCs (D). Values expressed as mean  $\pm$  standard deviation of three independent experiments. Statistical significance, with respect to control, indicated by \* ( $p < 0.05$ ).

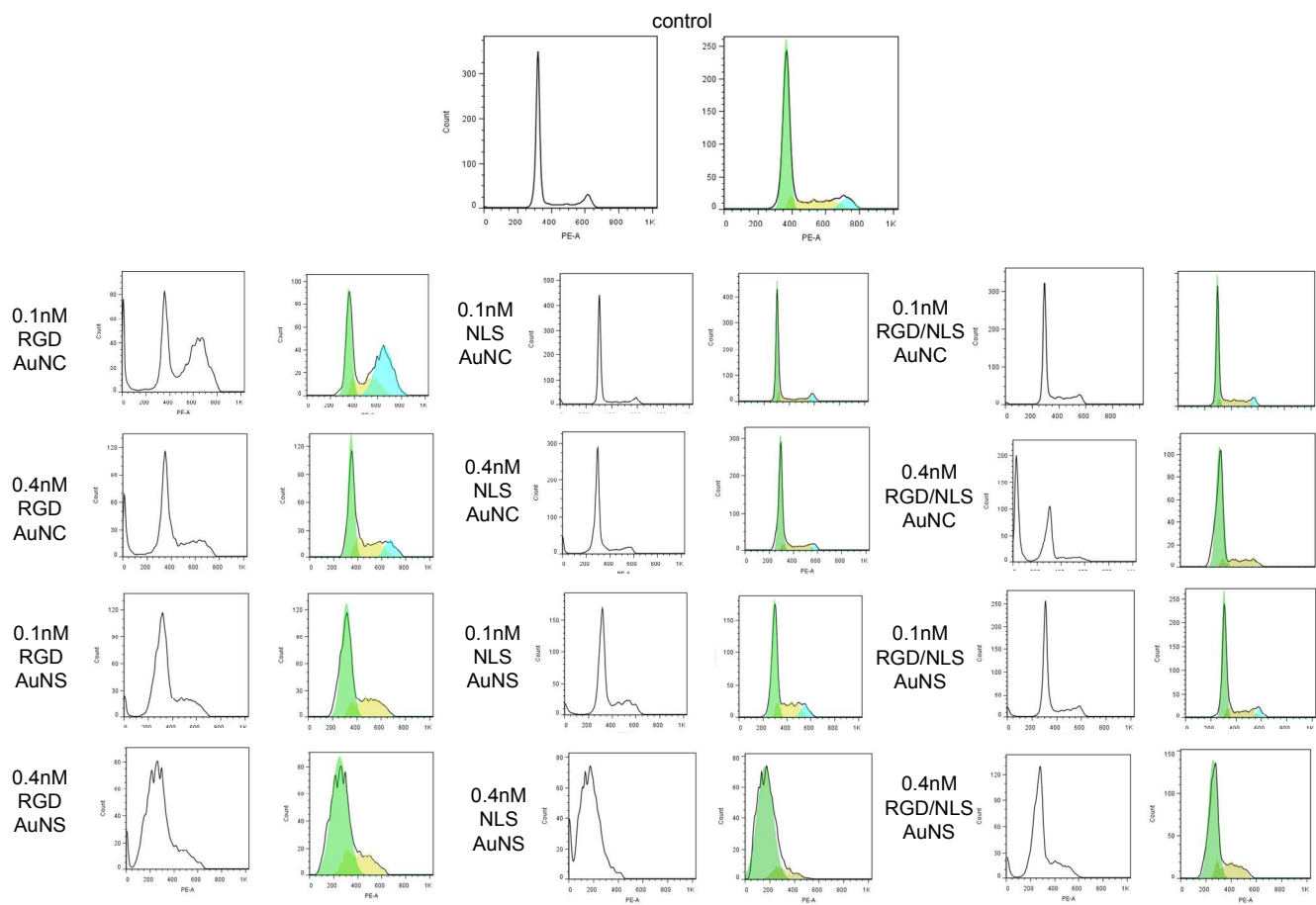


**Figure S3.** Raw data obtained from flow cytometry cell cycle analysis for all nanoparticle treatments tested in this work. Cell cycle histograms, not filled in, represent the raw data, including the subG1 population, indicative of an apoptotic population. SubG1 populations appear in HSC cells treated with 0.1 nM RGD-AuNC, 0.4 nM RGD-AuNC, 0.4 nM RGD-AuNS, 0.4 nM NLS-AuNS, 0.4 nM RGD/NLS-AuNS, and the greatest subG1 population in 0.4 nM RGD/NLS-AuNC. Cell cycle histograms, filled in, represent how the data was fit, after gating single cells and eliminating the subG1 populations, to obtain G0/G1 (green), S (yellow) and G2/M (blue) phase populations.

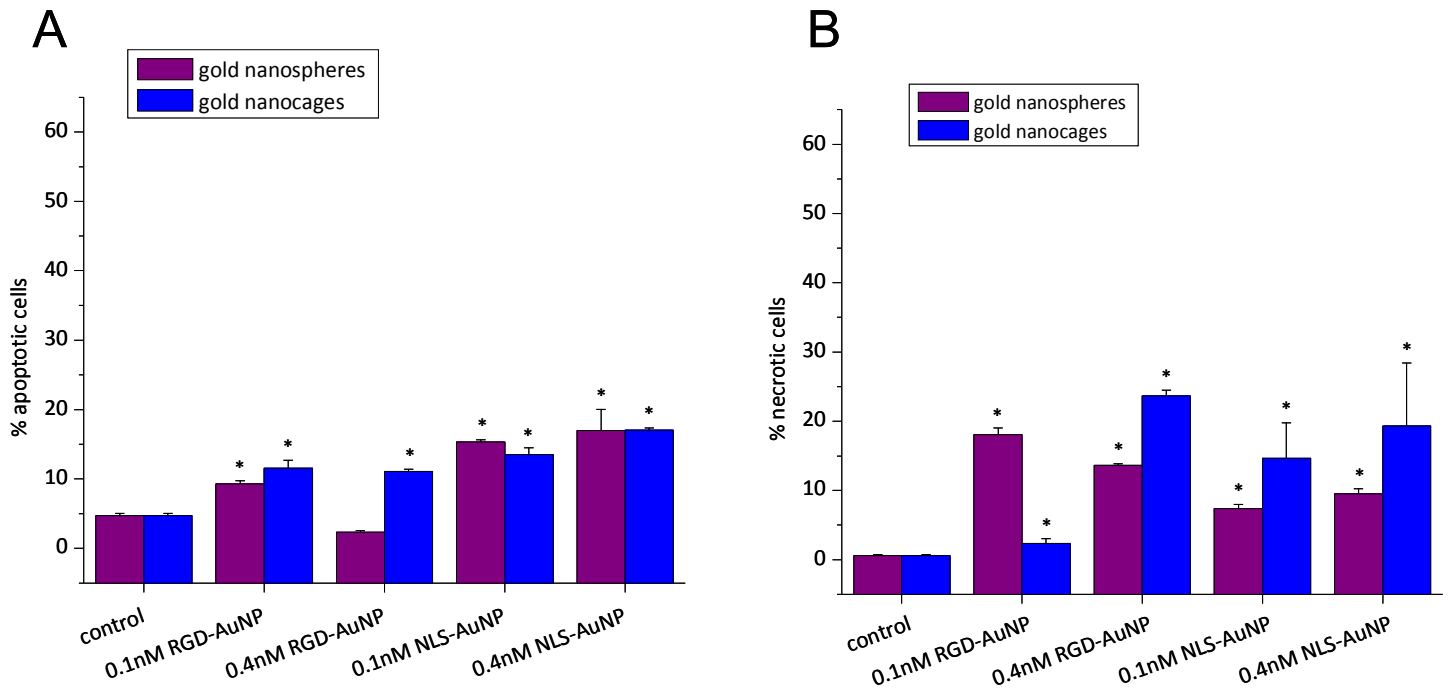


**Figure S4.** Peptide-conjugated gold nanoparticle-induced cell death, via apoptosis (A) and necrosis (B), in HSC cells after 48 h treatment with RGD-AuNSs, RGD-AuNCs, NLS-AuNSs, and NLS-AuNCs. Values expressed as mean  $\pm$  standard deviation of three independent experiments. Statistical significance, with respect to control, indicated by \* ( $p < 0.05$ ).

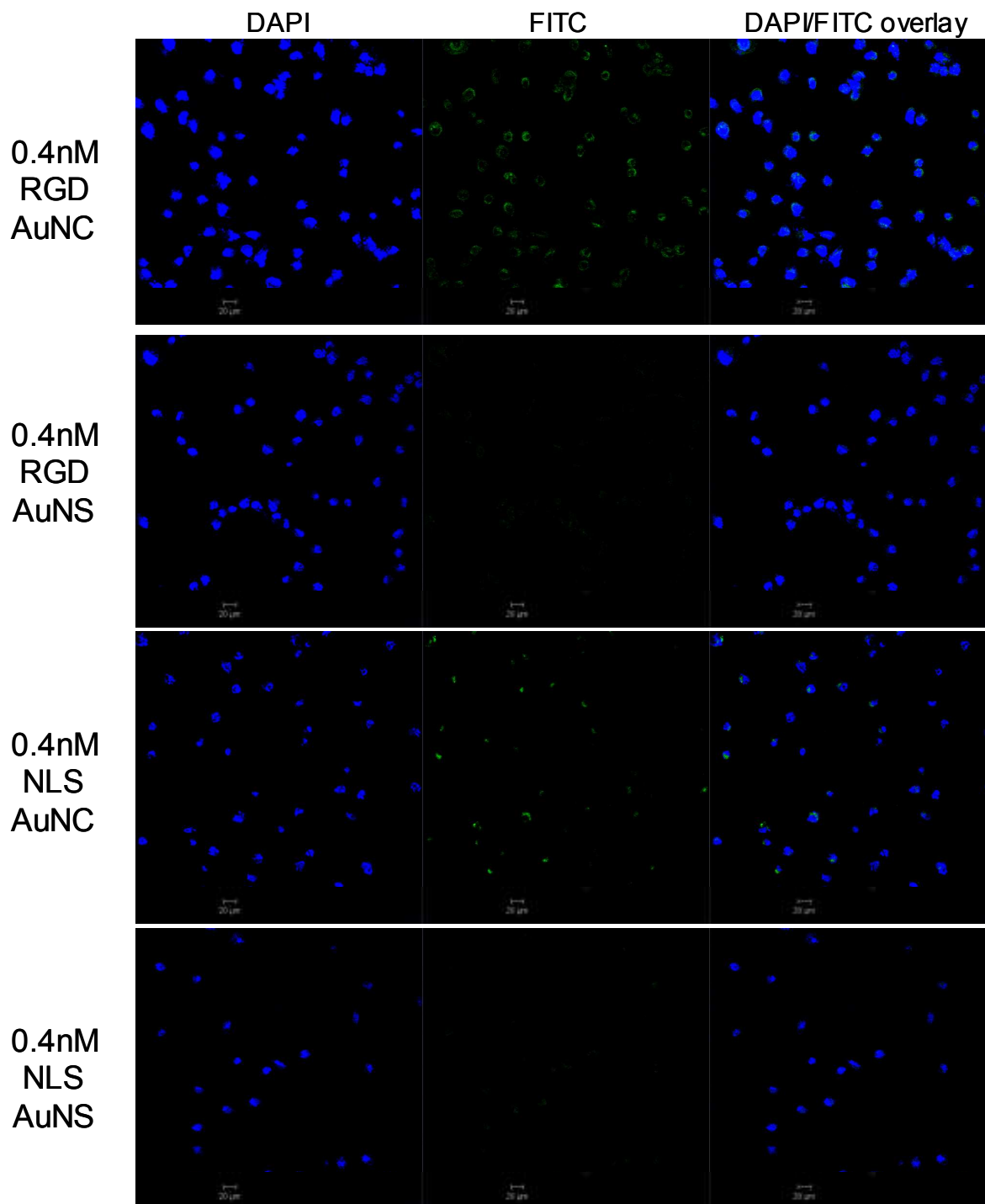


**Figure S5.** ROS generation detected by confocal microscopy for 0.4 nM RGD-AuNCs, RGD-AuNSs, NLS-AuNCs, and NLS-AuNSs. DAPI panel (left) shows the nuclei of HSC cells stained blue. FITC panel (middle) represents green fluorescence indicative of ROS generated inside cells. DAPI/FITC overlay (right) shows the combination of both nuclei and ROS. The 0.4 nM RGD-AuNCs and NLS-AuNCs display FITC fluorescence, indicating ROS are generated in HSC cells with this nanoparticle treatment. Scale bar: 20  $\mu$ m.

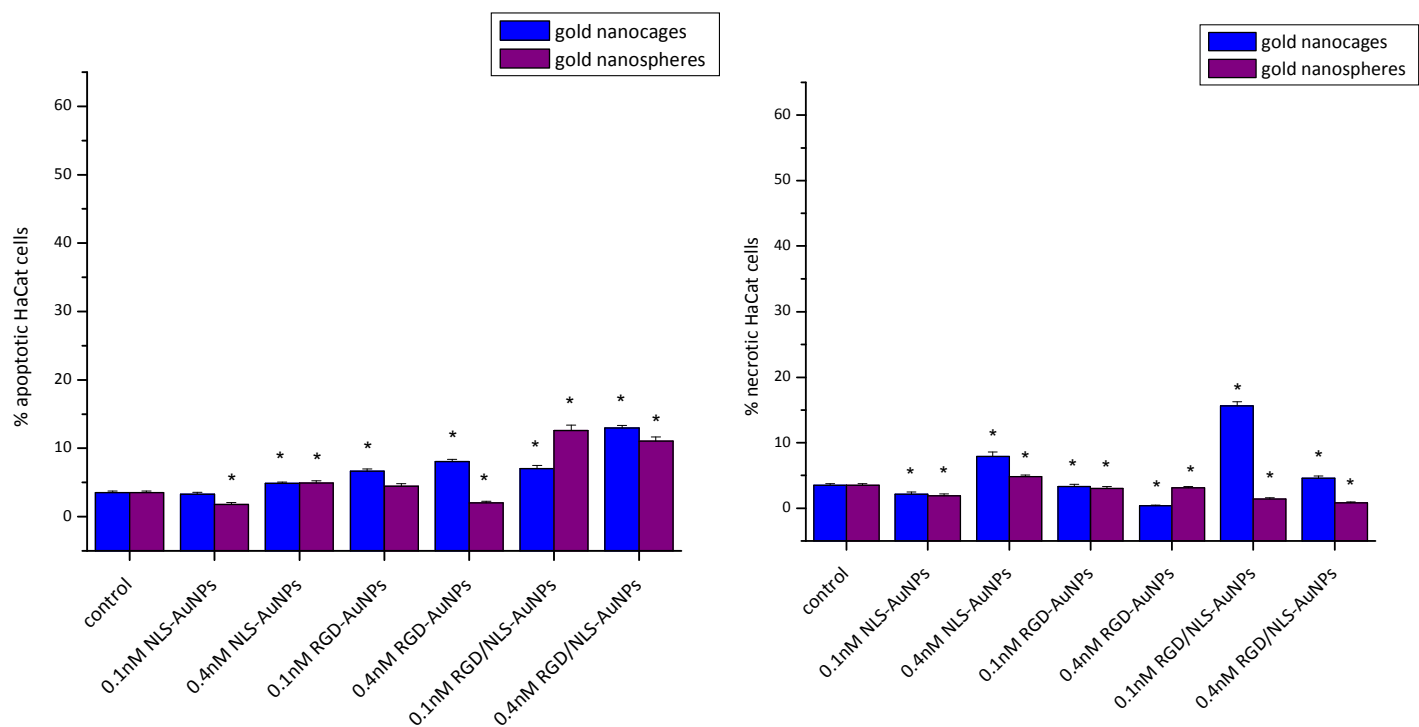


**Figure S6.** HaCat cell death via apoptosis (left) and necrosis (right) induced by all nanoparticle formulations. All nanoparticle formulations induce minimal cell death in the HaCat cells compared with the HSC cells. This was expected, as the HaCat cells do not overexpress the alpha beta integrins on their surface.<sup>1</sup> Values expressed as mean  $\pm$  standard deviation of three independent experiments. Statistical significance, with respect to control, indicated by \* ( $p < 0.05$ ).



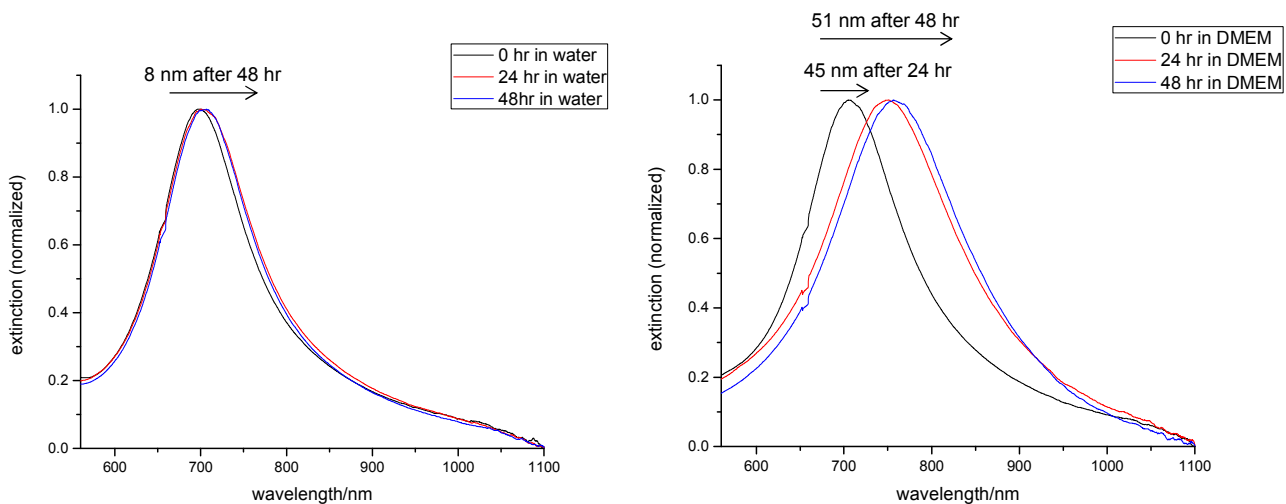


**Figure S7.** UV-Vis spectra of AuNCs in water (left) and DMEM, cell culture medium (right). A 51 nm shift in the surface plasmon of the AuNCs in DMEM is observed after 48 h at physiological conditions indicating the oxidation of silver atoms to  $\text{Ag}_2\text{O}$  on the inner cavity of the AuNC.

1. Koivisto, L., Larjava, K., Hakkinen, L., Uitto, V. J., Heino, J., and Larjava, H. (1999) Different integrins mediate cell spreading, haptotaxis and lateral migration of HaCaT keratinocytes on fibronectin, *Cell Adhes Commun* 7, 245-257.